J Neurophysiol 101: 2472–2484, 2009.
First published March 11, 2009; doi:10.1152/jn.91187.2008.

Noradrenergic Regulation of GABAergic Inhibition of Main Olfactory Bulb Mitral Cells Varies as a Function of Concentration and Receptor Subtype

Qiang Nai,[1] Hong-Wei Dong,[1] Abdallah Hayar,[2] Christiane Linster,[3] and Matthew Ennis[1]

[1]*Department of Anatomy and Neurobiology, University of Tennessee Health Science Center, Memphis, Tennessee;* [2]*Department of Neurobiology and Developmental Sciences, University of Arkansas for Medical Sciences, Little Rock, Arkansas; and* [3]*Department of Neurobiology and Behavior, Cornell University, Ithaca, New York*

Submitted 5 November 2008; accepted in final form 8 March 2009

Nai Q, Dong H-W, Hayar A, Linster C, Ennis M. Noradrenergic regulation of GABAergic inhibition of main olfactory bulb mitral cells varies as a function of concentration and receptor subtype. *J Neurophysiol* 101: 2472–2484, 2009. First published March 11, 2009; doi:10.1152/jn.91187.2008. The main olfactory bulb (MOB) receives a rich noradrenergic innervation from the pontine nucleus locus coeruleus (LC). Previous studies indicate that norepinephrine (NE) modulates the strength of GABAergic inhibition in MOB. However, the nature of this modulation and the NE receptors involved remain controversial. The goal of this study was to investigate the role of NE receptor subtypes in modulating the GABAergic inhibition of mitral cells using patch-clamp electrophysiology in rat MOB slices. NE concentration dependently and bi-directionally modulated $GABA_A$ receptor–mediated spontaneous and miniature inhibitory postsynaptic currents (sIPSCs/mIPSCs) recorded in mitral cells. Low doses of NE suppressed sIPSCs and mIPSCs because of activation of α2 receptors. Intermediate concentrations of NE increased sIPSCs and mIPSCs primarily because of activation of α1 receptors. In contrast, activation of β receptors increased sIPSCs but not mIPSCs. These results indicate that NE release regulates the strength of GABAergic inhibition of mitral cells depending on the NE receptor subtype activated. Functionally, the differing affinity of noradrenergic receptor subtypes seems to allow for dynamic modulation of GABAergic inhibition in MOB as function of the extracellular NE concentration, which in turn, is regulated by behavioral state.

INTRODUCTION

The locus coeruleus (LC)-noradrenergic system sends divergent efferent projections throughout the CNS with regional and laminar specificity (Lewis et al. 1987; McLean et al. 1989; Morrison et al. 1982; Proudfit and Clark 1991; Schuerger and Balaban 1999). This system has been implicated in pervasive but distinct functions such as modulation of behavioral state, attention, anxiety, and learning and memory (Robbins and Everitt 1982). The main olfactory bulb (MOB) receives a dense noradrenergic projection from LC that terminates in all but the most superficial layers (Shipley et al. 1985). Specifically, noradrenergic fibers preferentially target the internal plexiform layers (IPL) and granule cell layers (GCL), and to a lesser extent the mitral cell layer and external plexiform layer (EPL) (McLean et al. 1989). Generally paralleling this noradrenergic fiber distribution, each of the three major NE receptor subtypes (α1, α2, β) are expressed in multiple layers of the MOB, and individual MOB neurons seem to express multiple NE receptor subtypes (for review, see Ennis et al. 2007). For example, mitral cells express all three noradrenergic receptor subtypes and granule cells express α1 and α2 receptors (for review, see Ennis and Hayar 2008; Ennis et al. 2007).

The widespread distribution of noradrenergic fibers and receptors provides the structural basis for potentially diverse physiological functions of norepinephrine (NE) release in the MOB network. Indeed, behavioral studies in rodents have linked NE release and activation of the three noradrenergic receptor subtypes in the MOB to formation of conditioned odor preferences in neonates, as well as odor recognition and discrimination in mature animals (Doucette et al. 2007; Harley et al. 2006; Jiang et al. 1996; Mandairon et al. 2008; Sullivan et al. 2000; Veyrac et al. 2007). Diverse physiological effects of NE have been observed in the MOB, including modulation of EEG patterns during olfactory learning (Gray et al. 1986), direct excitation of mitral cells and facilitation of mitral cell responses to olfactory nerve input (Ciombor et al. 1999; Gire and Schoppa 2008; Hayar et al. 2001; Yuan et al. 2000), and enhancement of gamma frequency oscillations (Gire and Schoppa 2008).

Some of these observed behavioral effects of NE on olfactory processing may depend on modulation of GABAergic inhibition in MOB. However, somewhat discrepant effects have been reported on the direction and receptors involved in such modulation. Early observations in the turtle MOB indicated that NE disinhibited mitral cells, an effect attributed to direct inhibition of granule cells (Jahr and Nicoll 1982). A comparable conclusion—mitral cell disinhibition—was obtained in dissociated MOB cultures where NE, acting at α2 receptors, was reported to presynaptically inhibit mitral-to-granule cell synaptic transmission and vice versa (Trombley 1992; Trombley and Shepherd 1992). In contrast, field potential recordings suggested that NE infusion into MOB, acting at α1 but not α2 or β receptors, increased granule cell excitability (Mouly et al. 1995). A comparable conclusion was reached in the accessory OB where NE, acting via α1 receptors on granule cells, enhanced GABA release onto mitral cells (Araneda and Firestein 2006). In neonatal animals, OB infusions of β agonists decreased the paired-pulse depression of mitral cell–evoked granule cell layer field potentials (Wilson and Leon 1988), suggesting that β receptor activation suppresses glutamate release from mitral cells, perhaps decreasing granule cell mediated inhibition. LC stimulation, via activation of β receptors in the MOB, was reported to initially decrease and then increase paired-pulse depression of mitral cell–evoked field potentials in the granule cell layer (Okutani et al. 1998). It was concluded that NE release initially decreases and then in-

Address for reprint requests and other correspondence: Q. Nai, Dept. of Anatomy and Neurobiology, Univ. of Tennessee Health Science Ctr., 855 Monroe Ave., Suite 515, Memphis, TN 38163 (E-mail: qnai@utmem.edu).

creases mitral cell glutamate release onto granule cells. Other studies have reported that β receptor activation has no effect on GABAergic inhibition or dendrodendritic transmission between mitral and granule cells (Araneda and Firestein 2006; Trombley 1992; Trombley and Shepherd 1992).

Discrepancies among reported effects of NE on GABAergic inhibition may be caused by differences in species and/or experimental preparation. Another key factor may be differing pharmacological approaches (synaptic release of NE vs. exogenous NE application) or the concentration of NE used. In this regard, there are several crucial issues to be considered. LC neurons tend to exhibit synchronous activity (Berridge and Waterhouse 2003) and therefore LC activation will release NE globally throughout the MOB network. The location of NE receptors in relation to release sites, as well as rate of extracellular NE removal at the receptors, may exhibit variations. Therefore diffuse release of NE does not necessarily imply subsequent or equal activation of all NE receptor subtypes. LC discharge, and consequently extracellular NE levels, vary as a function of attentional state and level of vigilance (Berridge and Waterhouse 2003). The three NE receptor subtypes have differential affinities for NE (Ramos and Arnsten 2007). Therefore the net impact of NE release on the MOB network, including GABAergic inhibition, may be modulated as a function of the level of NE release and the specific NE receptors that are engaged by the prevailing extracellular concentration of NE.

The goals of this study were to determine whether and how the tonic level of GABAergic inhibition of MOB mitral cells varies with the extracellular concentration of NE and to determine the contribution of individual noradrenergic receptor subtypes to the observed influence of NE on this inhibition. Whole cell patch-clamp electrophysiology in rat MOB slices was used to study these questions. The results show that NE produces variable effects on GABAergic inhibition of mitral cells that vary as a function of NE concentration and actions of NE at multiple noradrenergic receptors.

METHODS

Slice preparation

Male and female Sprague-Dawley rats (P14–P30) were decapitated in accordance with Institutional Animal Care and Use Committee and National Institute of Health guidelines. Horizontal 400-μm-thick olfactory bulb slices were prepared as previously described (Dong et al. 2007). Briefly, the olfactory bulbs and a portion of the forebrain were dissected free from the surrounding skull, removed, and immersed in oxygenated chilled sucrose-artificial cerebrospinal fluid (ACSF) composed of (in mM) 26 NaHCO3, 1 NaH2PO4, 3 KCl, 4 MgSO4, 0.1 CaCl2, 20 glucose, and 234 sucrose; pH 7.3, 310 mOsm. Slices were cut using a Vibratome 3000 (Vibratome, St. Louis, MO) and transferred to an incubation chamber filled with normal ACSF saturated with 95% O_2-5% CO_2 and composed of (in mM) 124 NaCl, 26 $NaHCO_3$, 1 NaH_2PO_4, 3 KCl, 2 $MgSO_4$, 2 $CaCl_2$, 10 glucose, 0.4 ascorbic acid, and 2 sodium pyruvate (pH 7.3, 310 mOsm). Slices were held at 33°C for 15 min and then at room temperature (22°C) until used. For recording, a single slice was placed in a recording chamber and continuously perfused with ACSF equilibrated with 95% O_2-5% CO_2 at a rate of 1.5 ml/min.

Electrophysiology

Whole cell recordings were performed at 30°C. Neurons were visualized using an upright microscope (BX50WI, Olympus Optical, Tokyo, Japan) equipped with epifluorescence and near-infrared differential interference contrast (DIC) optics. Mitral cells were distinguished by soma location and by distinct electrophysiological and morphological properties (Dong et al. 2007). The recording pipette solution for voltage-clamp recordings contained (in mM) 120 cesium methanesulfonate, 1 NaCl, 10 phosphocreatine ditris salt, 3 Mg ATP, 0.3 GTP, 0.2 EGTA, 1 GDPβs, and 10 HEPES (pH 7.3, 290 mOsm); the G protein inhibitor GDPβs was included to prevent direct effects of NE and NE agonists on the recorded mitral cell (Hayar et al. 2001). The intracellular solution also contained 0.4% biocytin and 0.02% Lucifer yellow for visualization of the structural properties during recording and for future histological examination.

Inhibitory postsynaptic currents (IPSCs) were recorded in voltage-clamp mode at a holding potential of 0 mV. In these conditions (0 mV holding potential, low intracellular Cl^-), spontaneous IPSCs (sIPSCs) were recorded as outward currents as previously reported (Dong et al. 2007). To isolate miniature IPSCs (mIPSCs), TTX (1 μM) was included in the bath to block action potentials, and 2-amino-5-phosphonopentanoic acid (APV) and 6-cyano-2,3-dihydroxy-7-nitroquinoxaline (CNQX) were added to block ionotropic glutamate receptors.

Data analysis

Analog signals were low-pass filtered at 2 kHz (Axopatch 200B) and digitized at 5 kHz using a Digidata-1322A interface and pClamp 9 software (Axon Instruments). Detection of IPSCs as events was performed off-line using Mini Analysis program (Synaptosoft, Decatur, GA). Consecutive epochs of data (e.g., 12 ms) were searched for a peak current, and the average baseline current was calculated for an interval (e.g., between 3 and 4 ms) before the peak. The event amplitude was calculated by subtracting the average baseline current from the peak current, and the event was rejected if the amplitude did not exceed a given threshold (e.g., 10 pA). The times of occurrence of events were imported into Origin 7.0 (Microcal Software, Northampton, MA) for additional analysis. Dose-response relationships were generated by applying incremental doses (i.e., cumulatively) of NE or agonists in single cells. Drug concentrations producing a 50% increase or decrease in response (EC_{50} and IC_{50}, respectively) were determined from sigmoidal curves (Origin 7.0). Some dose-response curves were multiphasic and, in these cases, each phase was individually analyzed via sigmoidal curve fitting to determine EC_{50} or IC_{50}. Data, expressed as mean $\pm$ SE, were statistically analyzed using one-way repeated-measures ANOVA followed by post hoc comparisons (Newman-Keuls tests) or with Students *t*-test (SigmaStat, Aspire Software International, Ashburn, VA). Differences in IPSC frequency/amplitude distributions were analyzed using Kolmogorov-Smirnov (K-S) tests. Percentage data from different groups were analyzed with the Mann-Whitney *U* test.

Drugs

Drugs were applied by switching the bath perfusion solution with a three-way valve system. Isoproterenol (Isop), prazosin (Praz), clonidine (Clon), idazoxan (Idaz), propranalol (Prop), TTX, APV, and CNQX were obtained from Tocris Bioscience (Ellisville, MO). NE, phenylephrine (PE), gabazine, and other chemicals, if not specified otherwise, were purchased from Sigma (St. Louis, MO).

RESULTS

Triphasic effect of NE on sIPSC frequency

To study the effect of NE receptor activation on GABAergic inhibition of mitral cells, sIPSCs were recorded in normal

ACSF before and during bath application of NE at concentrations ranging from 0.01 μM to 3 mM (Fig. 1*A*). The basal sIPSC frequency and amplitude were 10.5± 1.2 Hz and 31.4± 1.7 pA (n = 54 cells), respectively. All sIPSC were eliminated by 10 μM gabazine (Fig. 1*A2*), confirming that they were caused by activation of GABAa receptors. As shown in Fig. 1*B*, NE dose-dependently modified the frequency of sIPSCs, resulting in a tri-phasic response profile: reduction at low doses, enhancement at intermediate doses, and relative suppression at high concentrations. The individual phases of the dose-response curve were individually analyzed (see METHODS; Fig. 1*C*). A significant reduction in sIPSC frequency occurred at low NE concentrations of 1.0–0.3 μM with an IC_{50} of 0.06 μM (Fig. 1*C1*). The sIPSC frequency at 0.1 μM NE was 85.6 ± 2.0% of control (n = 13; $P < 0.05$, ANOVA). At concentrations of 0.1–30 μM (Fig. 1*C2*), NE increased sIPSC frequency with an EC_{50} of 1.78 μM and a peak facilitatory effect at 30 μM (237.3 ± 53.8% of control; n = 13; $P < 0.05$, ANOVA). Increases >30 μM produced a decrease in sIPSC frequency toward baseline values with an IC_{50} of 167.3 μM (Fig. 1*C3*). For example, at 3 mM NE, the sIPSC frequency was 161.0 ± 32.9% of control, significantly lower than the frequency observed with intermediate NE concentrations (e.g., 30 μM).

Several control experiments were performed to assess the specificity of NE's effects. NE did not alter the detection of sIPSCs by changing the baseline current noise (Supplemental Fig. S1*A*).[1] To assess time-dependent deterioration of sIPSC frequency, we recorded from cells in control conditions when no drugs were applied. The frequency of sIPSCs exhibited minimal or no changes over recording periods comparable to those in the preceding experiment (Supplemental Fig. S1*C*). Changes in IPSC frequency were time-locked to NE application and were fully or partially reversible after washout (Supplemental Fig. S1, *E* and *F*). Taken together with the preceding results, these findings indicate that NE differentially modifies IPSC frequency in a concentration-dependent manner. The triphasic response profile may be caused by interaction of NE with different noradrenergic receptor subtypes, each with distinct affinity for NE.

Activation of α1 receptors increases sIPSCs

Two important questions are the threshold for NE's effects at the individual noradrenergic receptor subtypes, and the direction of influence of each subtype on GABAergic inhibition. To study the actions of NE at individual receptors, NE was applied at different concentrations in the presence of antagonists for two of the three NE receptors subtypes. To isolate and characterize NE's effects at the α1 receptor, NE

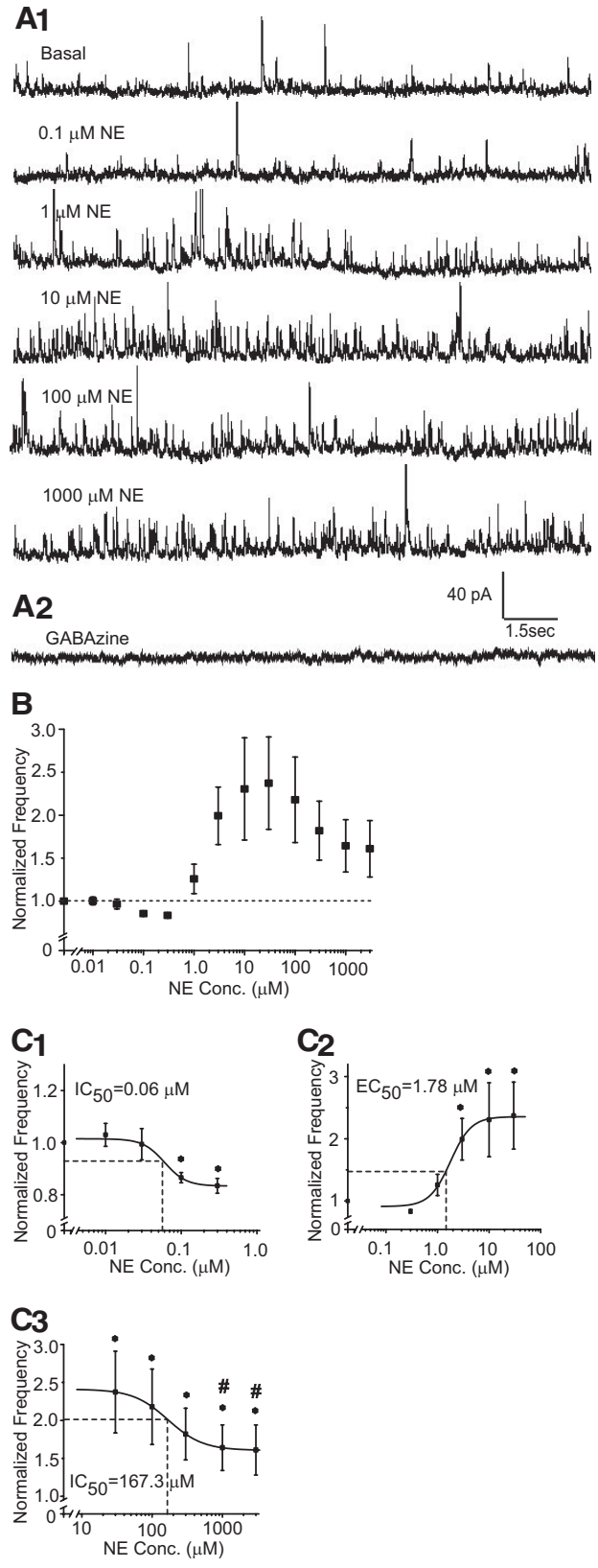

[1] The online version of this article contains supplemental data.

FIG. 1. Norepinephrine (NE) dose-dependently modulates spontaneous inhibitory postsynaptic current (sIPSC) frequency in mitral cells in normal artificial cerebrospinal fluid (ACSF). *A1*: voltage-clamp recordings showing sIPSCs recorded from a mitral cell before (Basal) and during bath application of NE from 0.01 μM to 1 mM. Small but detectable decrease in sIPSC frequency was seen at low concentrations (0.1–0.3 μM). NE from 1.0 to 30 μM increased sIPSC frequency, whereas the enhancement decreased at higher concentrations (>30 μM); all IPSCs were blocked by 10 μM gabazine (*A2*). *B*: cumulative NE dose-sIPSC frequency response curve (n = 13). *C1–C3*: individual concentration-sIPSC frequency response curves (sigmoidal fits) for the 3 components of the profile shown in *B*. The IC_{50} for the initial decrease was 0.06 μM (*C1*), the EC_{50} for the rising phase was 1.78 μM (*C2*), and the IC_{50} for the late decrease was 167.3 μM (*C3*). *$P < 0.05$ compared with control, ANOVA; #$P < 0.05$ compared with 30 μM, ANOVA. n = 6 −13 cells per group for all data in Fig. 1.

was applied in the presence of α2 and β receptor antagonists, idazoxan (Idaz, 10 μM) and propranalol (Prop,10 μM), respectively. Under these conditions (Fig. 2, *A* and *B*), NE produced an increase in sIPSC frequency that was significant at a threshold concentration of 10 μM and higher ($n = 6$; $P < 0.05$, ANOVA); the EC_{50} for this effect was 22.9 μM (Fig. 2, *A* and *B*). The increase in sIPSC frequency peaked at ~300 μM (554.8 ± 67.4% of control), and higher concentrations produced no further change (Fig. 2*B*). The increase of sIPSC frequency by 100 μM NE (416.1 ± 70.6% of control; $n = 8$; $P < 0.05$, ANOVA) was significantly reduced by the α1 receptor antagonist prazosin (Praz, 1 μM) to 167.3 ± 35.5% of control level (Fig. 2*C*); there was no difference in IPSC frequency in the Idaz + Prop versus Idaz + Prop + Praz + NE conditions ($P > 0.05$, ANOVA). Finally, there were no differences in the effects of NE at a given concentration when applied incrementally in a cumulative manner or at a single concentration. For example, there was no difference in sIPSC frequency in mitral cells when NE was applied incrementally to a concentration of 100 μM (normalized response, 4.46 ± 0.74; Fig. 2, *A* and *B*) versus when it was applied to drug-naïve mitral cells immediately in a single 100 μM application (4.16 ± 0.71; $P > 0.9$, Mann-Whitney *U* test). Thus there seemed to be no desensitization due to prolonged exposure to NE nor rundown of IPSC frequency during the cumulative-dose recording period. Taken together, these results indicate that NE acting at α1 receptors dose-dependently increases GABAergic sIPSCs in mitral cells.

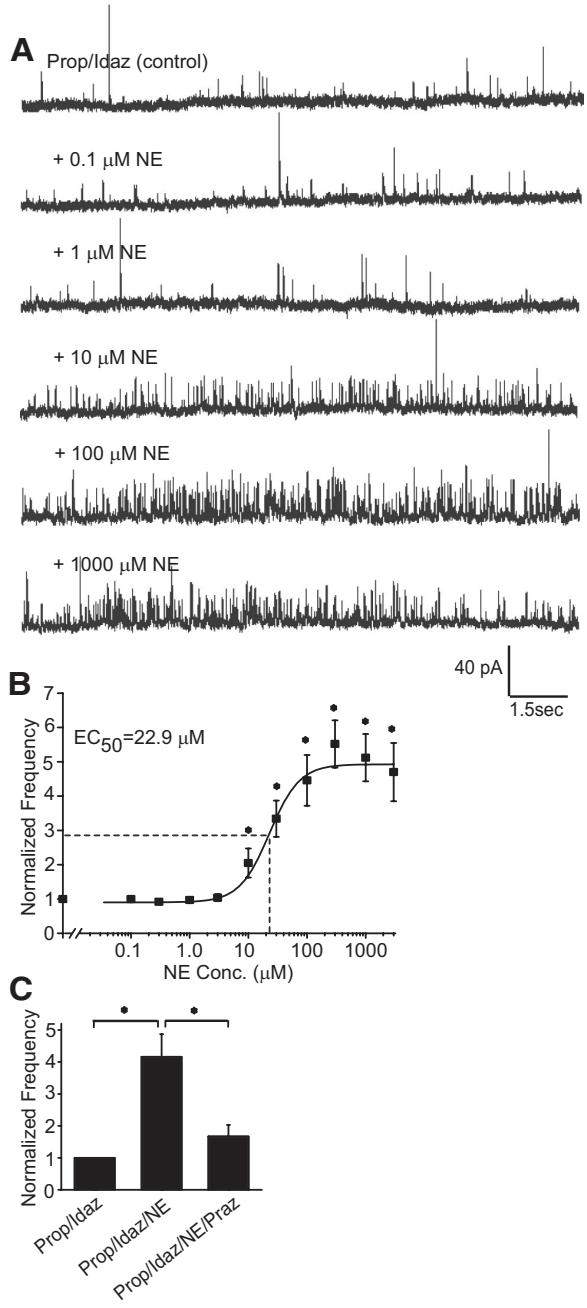

FIG. 2. NE-induced activation of α1 receptors increases sIPSCs. NE was applied in the presence of idazoxan (Idaz, 10 μM) and propranalol (Prop, 10 μM) to pharmacologically isolate α1 receptors. *A*: representative traces showing that activation of α1 receptors by NE increases the frequency of sIPSCs. *B*: NE dose-dependently increased sIPSCs frequency at a threshold value of 10 μM and an EC_{50} of 23 μM (*$P < 0.05$, ANOVA). *C*: in the presence of Prop/Idaz, the NE-induced (100 μM) increase in sIPSC frequency was reversed by 1 μM prazosin (Praz); *$P < 0.05$, ANOVA. There was no difference in IPSC frequency in the Idaz + Prop vs. Idaz + Prop + Praz + NE conditions ($P > 0.05$). $n = 6$–8 cells per group for all data in Fig. 2.

Activation of α2 receptors suppresses sIPSCs

The effect of α2 receptor activation on sIPSCs was determined by blocking α1 and β receptors with Praz and Prop, respectively (Fig. 3, *A* and *B*). In these conditions, sIPSCs were initially suppressed by low concentrations of NE. Significant inhibition occurred at a threshold of 0.1 μM NE (76.3 ± 4.4% of control; $P < 0.05$; $n = 8$) with maximal inhibition at 10 μM (46.6 ± 8.3% of control). However, the inhibition reversed at relatively high concentrations (≥30 μM), producing a return toward the initial pre-NE frequency (Fig. 3*B*); the highest concentration tested (3 mM) produced an increase in sIPSC frequency. This might be caused by competition of the high concentration of NE with α1 and β receptor blockers, which were applied at fixed concentrations. Fitting the initial portion of the concentration-response curve (0.01–30 μM) generated an IC_{50} of 0.12 μM (Fig. 3*C*). The decrease in sIPSC frequency by 10 μM NE (45.4 ± 3.1% of control; $n = 6$; $P < 0.05$, ANOVA) was reversed by Idaz (10 μM) to 89.2 ± 5.7% of control (Fig. 3*C*); there was no difference in IPSC frequency in the Praz + Prop versus Praz + Prop + Idaz + NE conditions ($P > 0.05$, ANOVA). These results indicate that NE acting at α2 receptors decreases GABAergic IPSCs in mitral cells, at least within estimated physiological ranges (see DISCUSSION).

Activation of β receptors enhances sIPSCs

The effect of β receptor activation on sIPSCs was determined during blockade of α1 and α2 receptors with Praz (1 μM) and Idaz (10 μM), respectively. NE concentration-dependently increased the frequency of sIPSCs (Fig. 4, *A* and *B*). A significant increase in sIPSC frequency was detected at a threshold of 0.03 μM NE (119.0 ± 4.6% of control; $n = 6$; $P < 0.05$, ANOVA), which is lower than the threshold concentration for NE actions at the α1 receptor (10 μM; Fig. 4*B*). Concentrations from 0.03 to 10 μM NE produced little additional effect, resulting in a plateau of the dose-response profile. However, at higher concentrations (>100 μM), further increases in sIPSC frequency were observed. Therefore only the initial portion of the concentration-response

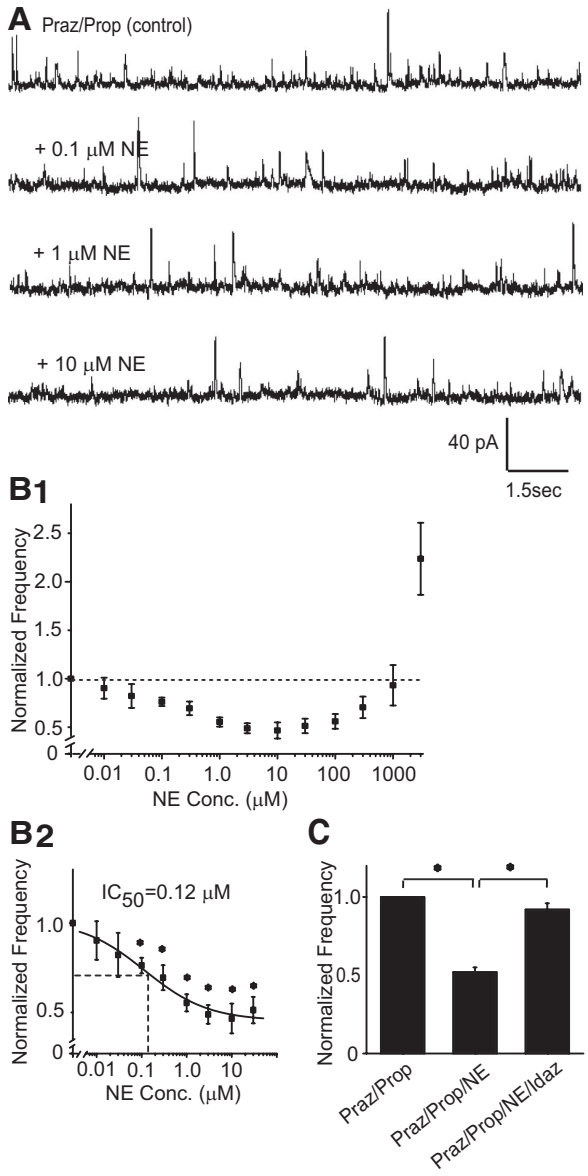

FIG. 3. NE-induced activation of $\alpha 2$ receptors inhibits sIPSCs. NE was applied in the presence of Praz (1 μM) and Prop (10 μM) to pharmacologically isolate $\alpha 2$ receptors. *A*: traces showing that, under these conditions, NE decreased sIPSC frequency. *B1*: Dose-response curve showing that NE decreased the frequency of sIPSCs from 0.01 to 10 μM, whereas IPSC frequency returned toward baseline with concentrations from 30 to 1,000 μM; note that the highest dose (3,000 μM) produced a large increase in sIPSC frequency. *B2*: concentration-sIPSC frequency response curve for the initial falling phase. The IC_{50} was 0.12 μM. *C*: in the presence of Praz/Prop, the decrease in sIPSC frequency by NE (10 μM) was reversed by 10 μM (Idaz, $^*P < 0.05$, ANOVA). $n = 6$ to 8 cells for all data in Fig. 3.

curve (0.01–10 μM NE) was fitted to generate EC_{50} (EC_{50} = 0.013 μM; Fig. 4*B2*). The magnitude of potentiation of sIPSCs by β receptor activation was less than that by $\alpha 1$ receptor activation. For example, the enhancement of sIPSC frequency via β receptor activation at 10 μM NE was 126.5 ± 5.7% of control (Fig. 4*B*) compared with 205.0 ± 42.5% of control for NE-$\alpha 1$ receptors (Fig. 2*B*). The increase in sIPSC frequency by 1 μM NE (124.1 ± 4.3% of control) was reversed by the β receptor antagonist Prop (10 μM) to 60.8 ± 6.8% of control level (Fig. 4*C*; $n = 6$; $P < 0.05$, ANOVA).

The effects of NE in the conditions above are compared in Fig. 9*A*. The average effect of NE, reconstructed by averaging its action at the three individual receptors, is also shown. Note that the average effect deviates from NE's profile in normal ACSF and is shifted to the right by approximately one order of magnitude. The reconstructed actions of NE may differ because of effects of the antagonists on basal IPSC frequency or because of facilitatory or synergistic effects when multiple receptor subtypes (e.g., $\alpha 1$ and β) are simultaneous engaged by NE as in normal ACSF.

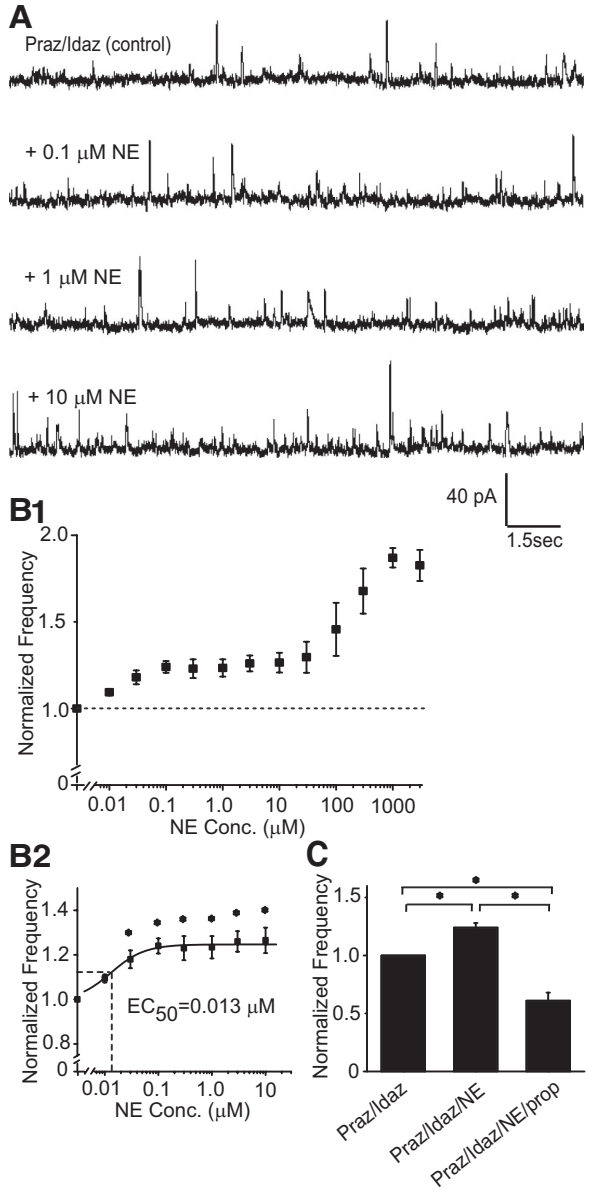

FIG. 4. NE-induced activation of β receptors increases sIPSCs. NE was applied in the presence of Praz (1 μM) and Idaz (10 μM) to pharmacologically isolate β receptors. *A*: traces showing that, under these conditions, NE increased the frequency of sIPSCs. *B1*: dose-response curve showing that NE increased the frequency of sIPSCs at all concentrations. *B2*: concentration-sIPSC frequency response curve for the initial rising phase. A significant increase was observed at a threshold of 0.03 μM NE and the EC_{50} was 0.013 μM. *C*: in presence of Praz/Idaz, the increase in sIPSC frequency induced by NE (1 μM) was reversed by Prop (10 μM); $^*P < 0.05$, ANOVA. $n = 6$ to 12 cells for all data in Fig. 4.

Effects of NE receptor agonists and antagonists on sIPSCs

To validate the effects of NE at individual receptor subtypes (α1, α2, and β) on sIPSCs, we studied the effects of receptor subtype specific agonists and antagonists (Fig. 5). As shown in Fig. 5*A*, the α1 receptor agonist phenylephrine (PE, 10 μM) and the β receptor agonist isoproterenol (Isop, 10 μM) increased sIPSCs frequency by 174.8 ± 19.6 and 136.3 ± 7.3% of control levels, respectively ($n = 6$; $P < 0.05$, paired *t*-tests). In contrast, the α2 receptor agonist clonidine (Clon, 10 μM) decreased sIPSC frequency to 65.0 ± 4.7% of control ($n = 5$; $P < 0.05$, paired *t*-test). These findings are in agreement with the direction of changes in sIPSC frequency produced by 0.1–30 μM NE at individual receptors (Figs. 2–4).

Application of individual NE receptor antagonists produced effects opposite to those produced by the agonists (Fig. 5*B*). Praz (1 μM) and Prop (β, 10 μM) decreased (47.5 ± 8.6 and 76.7 ± 2.4% of control, respectively; $n = 5$–6; $P < 0.05$, paired *t*-test), whereas Idaz (10 μM) increased sIPSC frequency (129.6 ± 4.3% of control; $n = 6$; $P < 0.05$, paired *t*-test). These results indicate that endogenous NE tonically modifies basal release of GABA and provide additional evidence that individual NE receptor subtypes exert differential effects on GABAergic inhibition of mitral cells.

α1 and α2 receptor activation by NE exerts opposing effects of mIPSCs

The studies to this point were conducted in normal ACSF to assess the effects of NE receptor activation on GABAergic inhibition when MOB network interactions are intact. A limitation of this approach is that observed changes in IPSCs may include both pre- and postsynaptic actions of NE. To isolate presynaptic effects of NE on GABA release, we next studied the effects of NE on mIPSCs in mitral cells recorded in the presence of TTX. Network interactions were further minimized by including the ionotropic glutamate receptor antagonists CNQX (20 μM) and APV (50 μM) in the bath. The basal mIPSC frequency and amplitude were 1.8 ± 0.2 Hz and 24.3 ± 1.2 pA ($n = 41$ cells), respectively. The basal frequency of mIPSCs was stable over 40-min recording periods (Supplemental Fig. S1*D*). Similar to the effects observed in normal ACSF (Fig. 1), NE exerted concentration-dependent effects on mIPSC frequency resulting in a tri-phasic profile (Fig. 6, *A* and *B*). A mild inhibition of mIPSCs was observed with low NE concentrations (0.01–1 μM), with significant suppression occurring at a threshold value of 0.03 μM (83.2 ± 4.0% of control; $n = 5$; $P < 0.05$, ANOVA) and extending to 1.0 μM (88.7 ± 3.0% of control; $n = 16$; $P < 0.05$, ANOVA). Concentrations from 3 to 30 μM produced a monotonic increase in mIPSC frequency (Fig. 6, *A* and *B*), with a peak response at 30 μM (282.0 ± 60.2% of control, $n = 16$, $P < 0.05$). As observed for sIPSCs in normal ACSF (Fig. 1), increases in NE beyond the concentration producing the peak effect were associated with a decrease toward baseline. For example, the mIPSC frequency with 100 μM NE was 190.2 ± 39.8% of control (Fig. 6*B*). Individual analyses of the three phases of the dose-response profile yielded an IC_{50} of 0.012 μM for the initial falling phase (Fig. 6*C1*), an EC_{50} of 2.76 μM for the rising phase (Fig. 6*C2*), and an IC_{50} of 123.2 μM for the high dose falling phase (Fig. 6*C3*). The values correspond well with those observed in normal ACSF (Fig. 1). As shown for 10 μM, the distribution of mIPSC interevent intervals and amplitudes (Fig. 6*D*) were shifted to the left by NE ($P < 0.001$ and $P < 0.05$, respectively, K-S tests); however, the average mIPSC amplitude was not altered ($P > 0.05$, ANOVA; $n = 16$). The increase in mIPSC frequency seems to be caused by an increase in intermediate size events, which in turn leads to the increase in intermediate amplitude events.

Voltage-gated Ca^{2+} channels (VGCCs) play important roles in mediating GABA release at granule cell-to-mitral cell dendrodendritic synapses and are involved in NE induced increases in mIPSC in accessory olfactory bulb mitral cells and acetylcholine-induced increases in MOB mitral cells (Araneda and Firestein 2006; Ghatpande et al. 2006). To study whether VGCCs are involved in NE-induced changes in mIPSC frequency, NE (10 μM) was applied in the presence of CNQX-APV-TTX and the VGCC blockers $NiCl_2$ (100 μM) and $CdCl_2$ (100 μM). In this condition, 10 μM NE failed to alter mIPSC frequency or mean amplitude ($n = 5$; $P > 0.05$, ANOVA; Fig. 7), indicating a critical role of VGCCs in the NE-mediated presynaptic regulation of GABA release.

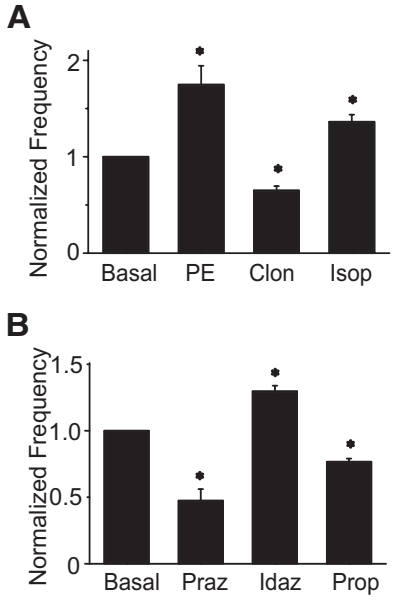

FIG. 5. Effects of NE receptor subtype–specific agonists and antagonists on sIPSCs. *A*: phenylephrine (PE, 10 μM) and isoproterenol (Isop, 10 μM) increased, whereas clonidine (Clon) decreased sIPSC frequency (*$P < 0.05$, paired *t*-test). *B*: prazosin (Praz, 1 μM) and propranolol (Prop, 10 μM) decreased, whereas idazoxan (Idaz, 10 μM) increased IPSC frequency (*$P < 0.05$, paired *t*-test). $n = 5$–6 for all groups.

α1 and α2 receptor agonists bi-directionally modulate mIPSC frequency

In normal ACSF, α1, α2, and β receptors were found to have different regulatory effects on sIPSCs. NE also dose-dependently regulated the frequency of mIPSCs. It is therefore reasonable to propose that each NE receptor subtype may differentially regulate the presynaptic release of GABA. To test this hypothesis, we examined the effects of individual NE receptor subtype–specific agonists on mIPSCs in mitral cells. The α1 receptor agonist PE dose-dependently increased mIPSC frequency from 1.0 to 30 μM, with a threshold of 3 μM ($n = 5$; $P < 0.05$, ANOVA) and an EC_{50} of 5.83 μM (Fig. 8,

A and *B*). As for NE, PE produced a leftward shift in the distribution of mIPSC interevent intervals ($P < 0.05$, K-S test) and amplitudes ($P < 0.05$, K-S test; data not shown) but did not affect mean mIPSC amplitude ($n = 5$; $P > 0.05$, ANOVA; data not shown). The mIPSC frequency peaked at 30 μM PE (296.2 ± 54.5% of control) but decreased toward baseline with further increases in concentration (i.e., ≥100 μM). This biphasic dose-response profile resembles that for the intermediate to high concentration relationship for NE's effect on IPSCs frequency in normal ACSF (Fig. 1) and in the presence of TTX (Fig. 6).

The α2 receptor agonist Clon decreased mIPSC frequency with an IC_{50} of 1.07 μM (Fig. 8, *C* and *D*). At 30 μM, Clon reduced mIPSC frequency to 52.8 ± 7.8% of control ($n = 5$; $P < 0.05$, ANOVA). This pattern corresponds well to the initial, low concentration inhibitory phase for NE's effect on spontaneous and miniature IPSCs (Figs. 1 and 6). Clon produced a significant rightward shift of the distribution of mIPSC interevent intervals ($P < 0.05$), consistent with the decreased frequency, but did not alter the distribution or the mean mIPSC amplitude ($P > 0.05$, K-S test and ANOVA; data not shown). Clon did not alter the detection of mIPSCs by changing the baseline current noise (Supplemental Fig. S1*B*). Finally, the β receptor agonist Isop did not change either the frequency or the amplitude of mIPSCs ($n = 5$; $P > 0.05$, ANOVA; Fig. 8, *E* and *F*; data for amplitude not shown), indicating that activation of β receptors does not directly modulate presynaptic GABA release.

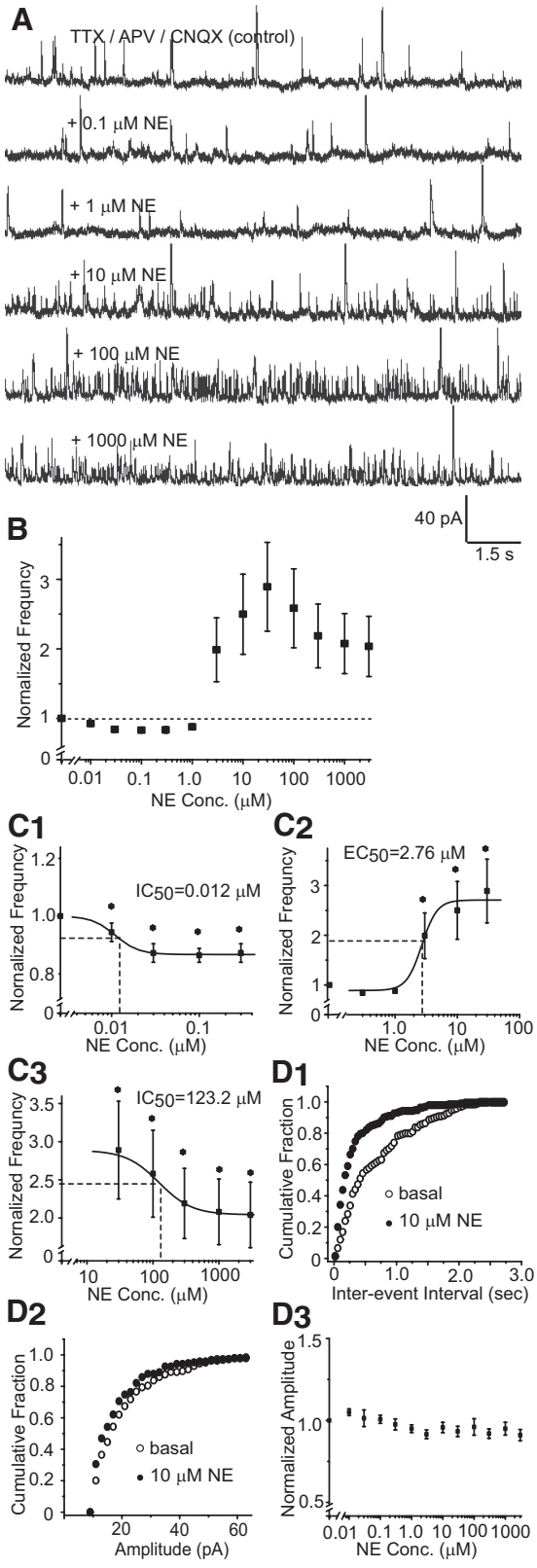

FIG. 6. NE-induced modulation of miniature IPSCs (mIPSCs). *A*: traces showing the effects of NE on mIPSCs in the presence of TTX (1 μM), 2-amino-5-phosphonopentanoic acid (APV; 50 μM), and 6-cyano-2,3-dihydroxy-7-nitro-quinoxaline (CNQX; 20 μM). *B*: dose-response curve showing that NE elicits a triphasic regulation of mIPSC frequency consisting of an initial decline, an intermediate dose facilitation, followed by a high dose reversal of the facilitation. *C1–C3*: individual concentration-sIPSC frequency response curves for the 3 components of the profile shown in *B*. The IC_{50} for the initial decrease was 0.012 μM (*C1*), the EC_{50} for the rising phase was 2.76 μM (*C2*), and the IC_{50} for the late decrease was 123.2 μM (*C3*); *$P <$ 0.05, ANOVA. *D*: the mIPSC interevent distribution for an example cell was shifted to the left by 10 μM NE (*D1*; $P < 0.001$, K-S test), as was the amplitude distribution (*D2*; $P < 0.05$, K-S test); mean mIPSC amplitudes were not significantly altered by NE (*D3*). $n = 5$ to 16 cells per group for data in Fig. 6.

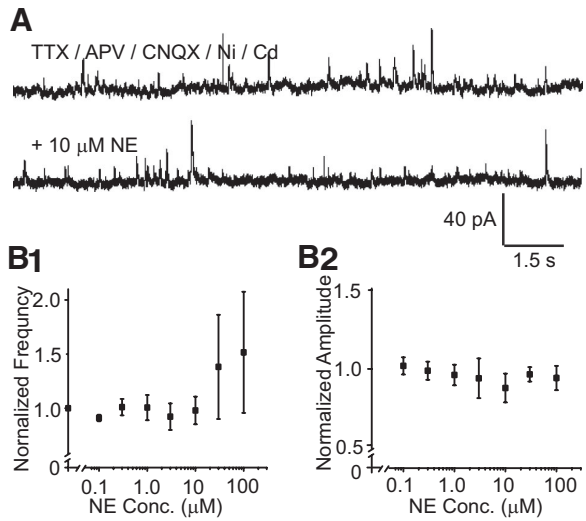

FIG. 7. NE-induced modulation of mIPSCs is blocked by Ca^{2+} channel antagonists. *A*: traces and group data showing that NE (10 μM)-evoked increases in mIPSC were blocked by prior application of the voltage-gated Ca^{2+} channel (VGCC) antagonists $NiCl_2$ (100 μM) and $CdCl_2$ (100 μM). *B*: in the presence of VGCCs, NE did not alter mean IPSC frequency (B1) or amplitude (B2); $P > 0.05$, ANOVA, $n = 5$.

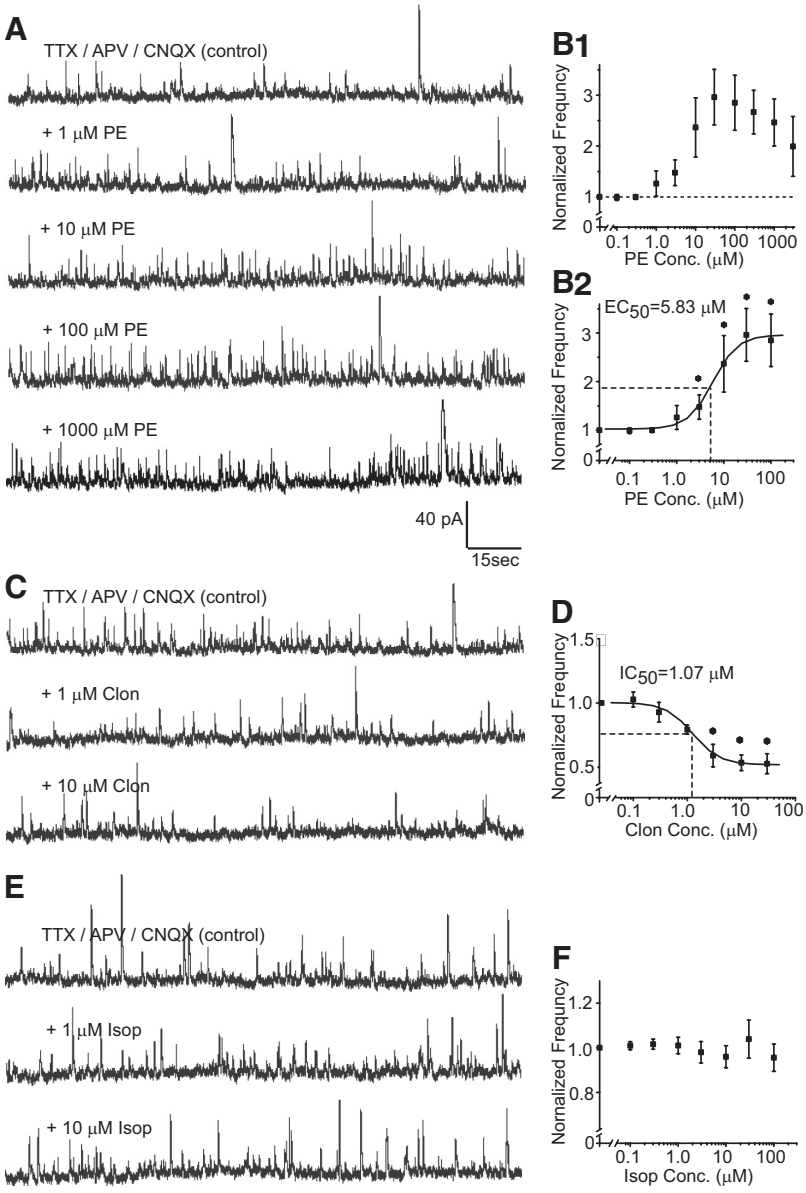

FIG. 8. α1 and α2 receptor activation exert opposing effects on mIPSCs. *A*: traces showing that PE increases mIPSC frequency in the presence of TTX (1 μM), APV (50 μM), and CNQX (20 μM). *B1*: dose-response curve showing that PE elicits a biphasic regulation of mIPSC frequency consisting of an initial increase followed by a decrease in the enhancement at higher concentrations. *B2*: dose-response curve for the initial rising phase (in *B1*) shows that PE increased mIPSC frequency with EC_{50} of 5.83 μM; $^*P < 0.05$, ANOVA. *C* and *D*: traces (*C*) and dose-response curve (*D*) showing that Clon suppressed mIPSC frequency with an IC_{50} of 1.07 μM; $^*P < 0.05$, ANOVA. *E* and *F*: traces (*E*) and dose-response curve (*F*) showing that Isop had no effect on mIPSC frequency; $P > 0.05$, ANOVA. Note: $n = 5$ cells per group for data in Fig. 8.

The effects of NE, PE, and Clon on mIPSC frequency are compared in Fig. 9*B*. Note the close correspondence between the profiles for NE and PE, with the exceptions of the low concentration inhibition observed for NE. This initial inhibitory phase corresponds well to the action of Clon.

DISCUSSION

The results of this study indicate that there is a triphasic relationship between extracellular levels of NE and the degree of tonic GABAergic inhibition of mitral cells as assessed by measurements of GABAa receptor–mediated IPSCs. Specifically, NE concentrations in the submicromolar range suppress both spontaneous and miniature IPSCs, whereas intermediate NE concentrations in the low micromolar range (1–30 μM) increase the frequency of IPSCs. Our pharmacological analyses indicated that low-dose IPSC suppression is mediated by activation of α2 receptors, whereas the intermediate dose facilitation is caused by α1 and β receptor activation. The α1 and α2 effects are presynaptically mediated, presumably by actions on granule cells, and were dependent on VGCCs. Concentrations $\geq$100 μM NE reversed the facilitation of IPSCs observed at intermediate doses. Taken together, these findings indicate that low levels of NE decrease spontaneous release of GABA, whereas higher concentrations associated with moderate to vigorous LC discharge lead to increased inhibition of mitral cells.

Methodological and neuroanatomical considerations

An important consideration is how well the mode of NE application used in this study relates to the pattern of NE release in the MOB during LC discharge. Anatomical and physiological findings suggest that LC discharge is likely to produce global release of NE throughout the MOB. LC fibers are particularly dense in the internal plexiform and granule cell layers (McLean et al. 1989), moderate in the external plexiform and mitral cell layers, and nearly absent in the glomerular

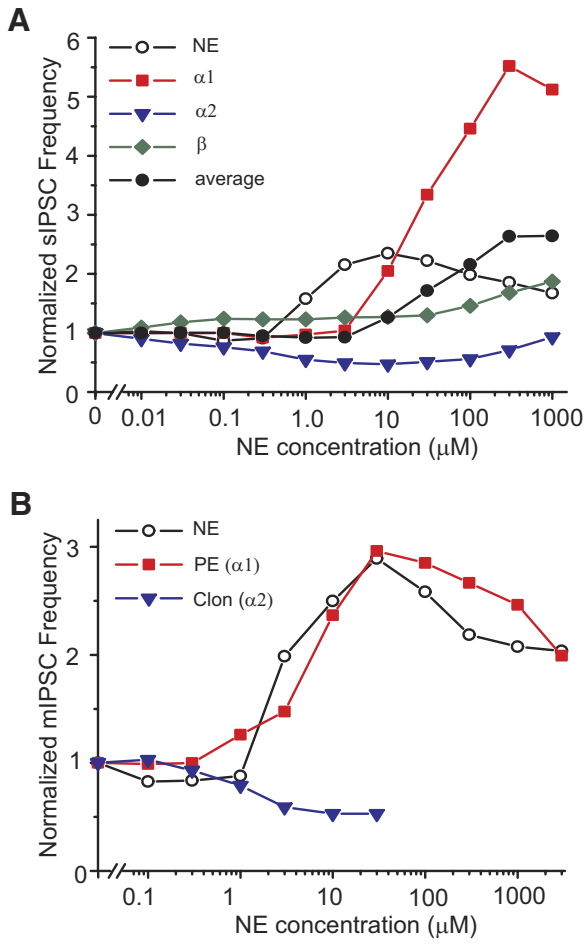

FIG. 9. *A*: summary plot comparing the dose-response relationship for NE's actions on sIPSCs in normal ACSF (NE) and at individual receptors when 2 receptors were blocked with antagonists. The average effect of NE, reconstructed by averaging its action at the 3 individual receptors, is also shown. Note that the average effect deviates from NE's profile in normal ACSF. *B*: plot comparing the effect of NE, PE, and Clon on mIPSCs. Note close correspondence between the effect of NE and PE, except for the initial low dose inhibition produced by NE.

layer. Although there are laminar gradients in the density of LC-NE fibers, it is clear that the innervation extends across the subglomerular layers (McLean et al. 1989). Similarly, NE receptors occur in multiple layers of the MOB and are expressed by multiple cell types, in general consistent with the pattern of NE fiber innervation (see Ennis et al. 2007 for review). Physiological studies showed that LC neurons, as a population, tend to fire synchronously tonically or in response to excitatory input (Aston-Jones and Bloom 1981; Berridge and Waterhouse 2003). Therefore even if individual LC neurons project with sublaminar specificity, functionally the parallel activity of the ensemble of LC neurons that project to MOB should lead to diffuse release of NE throughout this structure. Therefore the use of bath-applied NE in this study may approximate diffuse synaptic release of NE in MOB that occurs in vivo. However, bath application may differ in several critical aspects. First, the amount of NE released in the MOB in vivo may exhibit laminar differences that are proportional to the density of NE axon terminals. Second, the degree of receptor activation will ultimately depend on the proximity of the receptors to NE terminal release sites. In this study, all three NE receptor subtypes were equally exposed to the same concentration of NE, a condition that may not occur during synaptically evoked NE release.

Unfortunately, key data to assess these issues—subcellular localization of noradrenergic receptors in the MOB and their relationship to NE terminal release sites—are unavailable. However, these results that NE presynaptically modulates granule cell GABA release are consistent with findings that granule cells express α1 and α2 receptors (Day et al. 1997; Domyancic and Morilak 1997; McCune et al. 1993; Nicholas et al. 1993; Pieribone et al. 1994; Talley et al. 1996; Winzer-Serhan et al. 1997a,b). There are laminar differences in receptor subtype binding, with the density of α1 receptors reaching the highest levels in the brain in the external plexiform layer; the deeper MOB layers exhibit more moderate levels of α1 receptor binding (Sargent-Jones et al. 1985; Young and Kuhar 1980). In contrast, α2 receptor binding sites are particularly dense in the granule cell layer but are sparse in the more superficial layers (Holmberg et al. 2003; Young and Kuhar 1979). These findings may suggest that α1 receptors are more densely distributed to granule cell distal dendrites in the EPL, whereas α2 receptors are concentrated at granule cell proximal dendrites and somata. Such a differential distribution may underlie the more robust effects of α1 than α2 receptor activation on IPSC frequency in this study.

A second technical consideration is how the concentration range of exogenously applied NE in this study correlates with concentrations of synaptically released NE. In anesthetized animals where LC tonic firing rate averages 1–2 Hz, basal extracellular concentrations of NE in the olfactory bulb and prefrontal cortex have been reported in the 0.3- to 0.6-nM range (Berridge and Abercrombie 1999; El-Etri et al. 1999); prefrontal cortical NE levels are fivefold higher (i.e., 2.4 nM) in unanesthetized animals (Finlay et al. 1995). Tonic increases in LC discharge to 4–5 Hz in anesthetized animals are associated with increases in NE levels to ~2.4 nM, whereas phasic bursts of LC discharge or tonic firing rates of ≤15–20 Hz are associated with levels of 90 nM to 2 μM (Berridge and Abercrombie 1999; Devilbiss et al. 2006; El-Etri et al. 1999; Florin-Lechner et al. 1996). The IC_{50}s for NE's inhibition of spontaneous and miniature IPSCs were 60 (Fig. 1) and 10 nM (Fig. 6), which are somewhat higher than basal extracellular levels of NE in vivo. However, NE levels at synaptic release sites may be substantial higher than values obtained via in vivo microdialysis. Increased IPSCs were observed in normal media at a threshold of ~1.78 μM, which is within the range observed during vigorous LC discharge in vivo. Clearly, however, additional in vivo studies using LC activation to induce synaptic release of NE are needed to confirm the effects of NE on modulation of GABA release in the MOB in this study.

α2 RECEPTOR ACTIVATION INHIBITS IPSCS IN MITRAL CELLS. The overall dose-response profile for NE's actions on GABAergic inhibition of mitral cells was similar in the intact MOB network (sIPSC measurements) and when NE effects were restricted to neurons presynaptic to mitral cells (mIPSC measurements). In both conditions, the lowest concentrations of NE used reduced IPSC frequency with further increases in concentration producing an inverted-U profile characterized by an intermediate dose increase in IPSCs and a high dose decrease in IPSCs toward baseline level. Our pharmacological

analyses indicate that this overall profile is mediated by the combined actions of NE at individual noradrenergic receptor subtypes.

The lowest concentrations of NE (<1 μM) suppressed the frequency of IPSCs. The IC_{50} values for this inhibition were 0.06 and 0.012 μM for sIPSCs and mIPSCs, respectively. This suppression seems to be mediated by activation of α2 receptors because *1*) low concentrations of NE suppressed the sIPSC frequency when α1 and β receptors were blocked, and *2*) the α2 receptor agonist clonidine suppressed spontaneous and miniature IPSCs. Interestingly, in the absence of noradrenergic receptor antagonists, the NE-evoked decrease in IPSCs was relatively modest (~15% reduction) and observed over a narrow range of submicromolar concentrations (Figs. 1 and 6). However, when α1 and β receptors were blocked, the NE-evoked suppression was more robust (24–53% reduction) and extended to ~10 μM. This later profile is presumably caused by the absence of the IPSC stimulatory actions of α1 and β receptor activation that normally occur over this dose range. Several previous studies reported that NE decreased the frequency of GABAergic IPSPs in mitral cells, first in the turtle MOB (Jahr and Nicoll 1982) and later in rat MOB cultures (Trombley 1992, 1994; Trombley and Shepherd 1992). The receptor involved was not identified in the turtle study, whereas the effects of NE in the studies of Trombley were attributed to α2 receptor activation. However, the results of these studies were obtained with relatively high concentrations NE (30–100 μM) and are difficult to reconcile with increased IPSC frequency observed with similar concentrations in this study. Results from a more recent study in the accessory olfactory bulb indicated that α2 receptor activation with clonidine tended to decrease mIPSCs in mitral cells, although this trend was not statistically significant (Araneda and Firestein 2006). NE-induced suppression of mIPSCs may not have been detected in the study of Araneda and Firestein (2006) because NE concentrations of 3–30 μM were used.

α1 RECEPTOR ACTIVATION INCREASES IPSCS IN MITRAL CELLS. Concentrations of NE ranging from ~1 to 30 μM produced a dose-dependent increase in the frequency of IPSCs in mitral cells, with EC_{50} values of 1.8 and 2.8 μM for sIPSCs and mIPSCs, respectively. In normal ACSF, the increase seems to be mediated by combined actions of NE at both α1 and β receptors. The β receptor–mediated component (ascertained when NE was applied in the presence of α1 and α2 receptor antagonists) was associated with a plateau-like 25% increase sIPSCs with an initial EC_{50} of 0.013 μM. The α1 receptor-mediated facilitatory threshold and EC_{50} values (~5 and 23 μM, respectively) for sIPSCs were higher than those for the β receptor. β receptor agonists, however, did not affect mIPSCs, indicating that β effects on sIPSCs are not caused by direct actions on granule cell dendrites or other inhibitory interneurons presynaptic to mitral cells. This indicates that the facilitatory effect of 1–30 μM NE on mIPSCs is entirely caused by α1 receptor activation, a finding supported by the similar action of the α1 agonist PE. Intriguingly, the reversal of the facilitation of spontaneous and miniature IPSCs that occurs with NE concentrations in excess of 30 μM was replicated by high concentrations of PE. This seems to account for the declining phase of inverted-U function at high NE concentrations. The reason for this is unclear, but it may be mediated by α1 receptor desensitization, excessive depolarization of granule cells, or nonspecific effects of NE or PE at these concentrations.

The NE-induced, α1 receptor-mediated enhancement of GABAergic inhibition is entirely consistent with results in accessory olfactory bulb mitral cells reported by Araneda and Firestein (2006). That study found that 3–30 μM NE or the α1 receptor agonist PE (30 μM) robustly increased the frequency of mIPSCs. Our lack of effect of β receptor activation on mIPSCs in MOB mitral cells is also consistent with the results in the accessory olfactory bulb (Araneda and Firestein 2006). These results and those of Araneda and Firestein (2006) suggest that activation of α1 receptors directly increases the excitability of granule cells, leading to increased GABA release. This is in agreement with findings in vivo that NE (0.1–1 mM) infusion into MOB, acting at α1 but not α2 or β receptors, increased granule cell excitability as assessed with field potential recordings (Mouly et al. 1995).

As noted above, β receptor agonists increased spontaneous but not miniature IPSCs in mitral cells recorded in the presence of TTX. These results suggest that direct activation of β receptors on granule cells is not sufficient to drive dendritic release of GABA, at least in the presence of TTX. The increase in sIPSCs in normal media was likely a secondary consequence of increased glutamatergic input to granule cells. Several observations support this possibility. Granule cells express relatively low levels of β receptors, and expression is only observed in subsets of granule cells (Booze et al. 1989; Palacios and Kuhar 1982; Wanaka et al. 1989; Woo and Leon 1995; Yuan et al. 2003). β receptor expression, however, seems to be more robust in mitral and tufted cells (Yuan et al. 2003). NE (1–30 μM) and β receptor agonists (10 μM Isop) have been reported to increase glutamatergic spontaneous excitatory postsynaptic currents (sEPSCs) and long-lasting depolarizations in mitral cells in vitro, an effect blocked by TTX (Gire and Schoppa 2008; Hayar et al. 2001). Taken together, these results suggest that β receptor activation enhances spike-driven glutamate release from mitral/tufted cells, which would in turn increase granule cell excitability and GABA release. Conflicting effects of the β receptor have been previously observed in vivo. In neonatal animals, β receptor stimulation in MOB decreased the lateral olfactory tract (LOT)-evoked, paired-pulse inhibition of granule cell field potentials (Wilson and Leon 1988). A subsequent study reported that LC stimulation initially decreased and subsequently increased paired-pulse depression of granule cell field potential responses evoked by LOT stimulation (Okutani et al. 1998). These effects were attributed to activation of β receptors. Changes in paired-pulse responses are indicative of changes in presynaptic transmitter release: increased PPD indicates presynaptic enhancement, and decreased PPD indicates suppression, of release. Accordingly, the results would suggest that NE-mediated activation of β receptors in neonates suppresses glutamate release from mitral/tufted cells (Wilson and Leon 1988) or decreases, then increases glutamate release (Okutani et al. 1998). Differences between these two studies may be due to age and/or degree of NE release produced by LC stimulation.

Our results that NE presynaptically modulates granule cell GABA release are consistent with previous findings that granule cells express α1 and α2 receptors as determined by immunocytochemistry and in situ hybridization (Day et al. 1997;

Domyancic and Morilak 1997; McCune et al. 1993; Nicholas et al. 1993; Pieribone et al. 1994; Talley et al. 1996; Winzer-Serhan et al. 1997a,b). However, there are laminar differences as based on receptor binding, with the density of α1 receptors reaching the highest levels in the brain in the EPL; the deeper MOB layers exhibit more moderate levels of α1 receptor binding (Sargent-Jones et al. 1985; Young and Kuhar 1980). In contrast, α2 receptor binding sites are particularly dense in the granule cell layer and spare in the more superficial layers (Holmberg et al. 2003; Young and Kuhar 1979). These findings may suggest that α1 receptors are more densely distributed to granule cell distal dendrites in the EPL, whereas α2 receptors are concentrated at granule cell proximal dendrites and somata. Such a differential distribution may underlie the more robust effects of α1 receptor activation on IPSC frequency in this study.

Functional considerations

Recordings of LC neurons in behaving animals have provided important insights into how NE release may impact on vigilance and sensory processing (see Berridge and Waterhouse 2003 for review). LC neurons in awake animals fire in two modes: tonic and phasic. Tonic firing rates, which vary over a limited range (2 ± 2 Hz), change with, and anticipate, arousal state transitions: activity is highest during active waking (>2 Hz) and decreases progressively with shifts to quiet waking (<2 Hz), slow wave sleep (<1 Hz), and REM sleep (silent). Brief phasic bursts of LC discharge occur in response to novel or salient environmental stimuli. Neurochemical studies have shown that there is a progressive increase in extracellular NE levels across this firing range, with maximal levels produced by simulated phasic bursts of LC discharge (Berridge and Abercrombie 1999; Devilbiss et al. 2006; El-Etri et al. 1999; Florin-Lechner et al. 1996). Behavioral studies in primates indicate that there is an inverted-U relationship between LC firing rates across the range mentioned above and vigilance in visual discrimination tasks (Aston-Jones et al. 1994), a relationship similar to that observed here for NE-evoked modulation of IPSCs.

Our findings suggest that low concentrations of NE in the bulb decreased IPSCs, an effect that would lead to disinhibition of mitral cells. This suggests that low level increases in NE release, perhaps those achieved by low tonic LC firing rates, may be associated with mitral cell disinhibition. Functionally, this would tend to render mitral cells more sensitive to odors. However, the cost of this increased sensitivity would be reduced ability to discriminate among odorants. In other words, reduced granule to mitral cell inhibition may improve the sensitivity of an individual mitral cell to an odor to which it is well tuned to, but it would also render that cell more responsive to concentrations of odors that it is less well tuned to (i.e., odors with a low affinity for the receptor cells projecting to the same glomerulus). As a consequence, its molecular receptive field would increase (Linster and Gervais 1996; Linster and Hasselmo 1997). Intriguingly, behavioral studies have yet to identify an effect of α2 receptor modulation on olfactory processing. Systemic injections of α2 receptor agonists do not seem to alter conditioned odor preferences in neonates (Harley et al. 2006). In adult rats, α2 receptor blockade in the MOB did not impair spontaneous odor discrimination (Mandairon et al. 2008). Additional behavioral studies are needed to determine whether α2 receptor–mediated disinhibition of mitral cells modulates odor sensitivity thresholds.

Further increases in the NE concentration to the low μM level in this study were associated with increased levels of IPSCs in mitral cells via activation of α1 receptors. This suggests that elevated levels of NE release, perhaps during bursts of LC activity or higher tonic LC firing rates, would lead to a net increase in GABAergic inhibition of mitral cells. At these NE levels, we speculate that the α1 receptor stimulatory effect overrides the α2 receptor inhibitory effect on granule cell GABA release. It is noteworthy that NE concentrations in the low micromolar range also directly excite mitral cells (Hayar et al. 2001). Functionally, it is possible that the direct α1 receptor–mediated increase in mitral cell excitability, combined with the direct increase in α1 receptor–mediated GABAergic inhibition, may render the mitral cells more sensitive to weak odors by bringing them closer to spike threshold, while at the same time preserving or even increasing lateral inhibition. What are the possible functional correlates of such actions? Enhanced mitral cell excitability with a parallel increase GABAergic inhibition may function to increase odor sensitivity while preserving discriminability. Alternatively, a simultaneous increase of excitation and inhibition could increase the oscillatory synchronization in the mitral cell-granule cell feedback loop. Increased oscillations would enhance synchronization of mitral cell discharge, which has been proposed to enhance contrast at the output level of the MOB (Cleland and Linster 2002; Linster and Cleland 2001). In this regard, it is noteworthy that NE application in MOB slices has recently been reported to enhance olfactory nerve-evoked gamma-frequency oscillations (Gire and Schoppa 2008). Recent behavioral studies have indicated that α1 receptor activation enhances odor discrimination. Blockade of α1 receptors in the MOB was found to impair spontaneous discrimination between pairs of chemically and perceptually similar odorants (Mandairon et al. 2008). Combined blockade of both α1 and β receptors in MOB has also been reported to impair learning in reward-motivated odor discrimination testing paradigms using two closely related odorants (Doucette et al. 2007; Mandairon et al. 2008).

Finally, it is noteworthy that the inverted-U dose-response relationship observed here for NE's modulation of IPSC frequency in mitral cells is similar to that observed in previous cellular and behavioral studies of NE function. This pattern is observed for the degree of LC activation or NE concentration and modulation of thalamic and cortical neuronal excitability and signal-to-noise ratios in vitro and in vivo (Berridge and Waterhouse 2003; Devilbiss and Waterhouse 2000, 2004; Devilbiss et al. 2006; Waterhouse et al. 1998). Notably, there is an inverted-U relationship between NE concentration and the frequency of GABAergic IPSCs in frontal cortex neurons similar to the profile described here (Kawaguchi and Shindou 1998). As noted earlier, behavioral studies in primates indicate that there is an inverted-U relationship between LC firing rates (and presumably NE release) and vigilance in visual discrimination tasks. Performance is poor with low LC discharge and optimal with intermediate discharge levels associated with focused attention (Aston-Jones et al. 1994). At the highest levels of tonic LC discharge, associated with scanning or labile attention, performance is again poor, but it is thought that these

LC discharge rates are important in situations requiring high behavioral flexibility rather than focused attention. In neonatal rats, there is an inverted-U relationship between the level of $\alpha 1$ or β receptor activation in the MOB and the degree of conditioned odor preferences (Harley et al. 2006). The differential affinities of noradrenergic receptor subtypes may allow for differential modulation of GABA release and olfactory processing as a function of the level of NE release, which in turn, is regulated by behavioral state (Berridge and Waterhouse 2003).

GRANTS

This study was supported by National Institutes of Health Grants DC-008702 (CRCNS Award Program), DC-06356, DC-07123, DC-03195, and RR-020146.

REFERENCES

Araneda RC, Firestein S. Adrenergic enhancement of inhibitory transmission in the accessory olfactory bulb. *J Neurosci* 26: 3292–3298, 2006.

Aston-Jones G, Bloom FE. Norepinephrine-containing locus coeruleus neurons in behaving rats exhibit pronounced responses to non-noxious environmental stimuli. *J Neurosci* 1: 887–900, 1981.

Aston-Jones G, Rajkowski J, Kubiak P, Alexinsky T. Locus coeruleus neurons in monkey are selectively activated by attended cues in a vigilance task. *J Neurosci* 14: 4467–4480, 1994.

Berridge C, Waterhouse B. The locus coeruleus-noradrenergic system: modulation of behavioral state and state-dependent cognitive processes. *Brain Res Brain Res Rev* 42: 33–84, 2003.

Berridge CW, Abercrombie ED. Relationship between locus coeruleus discharge rates and rates of norepinephrine release within neocortex as assessed by in vivo microdialysis. *Neuroscience* 93: 1263–1270, 1999.

Booze RM, Crisostomo EA, Davis JN. Species differences in the localization and number of CNS beta adrenergic receptors: rat versus guinea pig. *J Pharmacol Exp Ther* 249: 911–920, 1989.

Castillo PE, Carleton A, Vincent J-D, Lledo P-M. Multiple and opposing roles of cholinergic transmission in the main olfactory bulb. *J Neurosci* 19: 9180–9191, 1999.

Ciombor KJ, Ennis M, Shipley MT. Norepinephrine increases rat mitral cell excitatory responses to weak olfactory nerve input via alpha-1 receptors in vitro. *Neuroscience* 90: 595–606, 1999.

Cleland TA, Linster C. How synchronization properties among second-order sensory neurons can mediate stimulus salience. *Behav Neurosci* 116: 212–221, 2002.

Day HE, Campeau S, Watson SJ Jr, Akil H. Distribution of alpha 1a-, alpha 1b- and alpha 1d-adrenergic receptor mRNA in the rat brain and spinal cord. *J Chem Neuroanat* 13: 115–139, 1997.

Devilbiss DM, Page ME, Waterhouse BD. Locus ceruleus regulates sensory encoding by neurons and networks in waking animals. *J Neurosci* 26: 9860–9872, 2006.

Devilbiss DM, Waterhouse BD. Norepinephrine exhibits two distinct profiles of action in sensory cortical neuronal responses to excitatory stimuli. *Synapse* 37: 273–282, 2000.

Devilbiss DM, Waterhouse BD. The effects of tonic locus ceruleus output on sensory-evoked responses of ventral posterior medial thalamic and barrel field cortical neurons in the awake rat. *J Neurosci* 24: 10773–10785, 2004.

Domyancic AV, Morilak DA. Distribution of alpha1A adrenergic receptor mRNA in the rat brain visualized by in situ hybridization. *J Comp Neurol* 386: 358–378, 1997.

Dong HW, Hayar A, Ennis M. Activation of group I metabotropic glutamate receptors on main olfactory bulb granule cells and periglomerular cells enhances synaptic inhibition of mitral cells. *J Neurosci* 27: 5654–5663, 2007.

Doucette W, Milder J, Restrepo D. Adrenergic modulation of olfactory bulb circuitry affects odor discrimination. *Learn Mem* 14: 539–547, 2007.

El-Etri MM, Griff ER, Ennis M, Shipley MT. Evidence for cholinergic regulation of basal norepinephrine release in the rat olfactory bulb. *Neuroscience* 93: 611–617, 1999.

Ennis M, Hamilton KA, Hayar A. Neurochemistry of the main olfactory system. In: *Handbook of Neurochemistry and Molecular Neurobiology* (3rd ed.), edited by Lajtha A. Heidelberg, Germany: Springer, 2007, vol. 20, p. 137–204.

Ennis M, Hayar A. *Physiology of the Olfactory Bulb, The Senses: A Comprehensive Reference/* San Diego, CA: Academic Press, 2008, vol. 4.

Finlay JM, Zigmond MJ, Abercrombie ED. Increased dopamine and norepinephrine release in medial prefrontal cortex induced by acute and chronic stress: effects of diazepam. *Neuroscience* 64: 619–628, 1995.

Florin-Lechner SM, Druhan JP, Aston-Jones G, Valentino RJ. Enhanced norepinephrine release in prefrontal cortex with burst stimulation of the locus coeruleus. *Brain Res* 742: 89–97, 1996.

Ghatpande AS, Sivaraaman K, Vijayaraghavan S. Store calcium mediates cholinergic effects on mIPSCs in the rat main olfactory bulb. *J Neurophysiol* 95: 1345–1355, 2006.

Gire DH, Schoppa NE. Long-term enhancement of synchronized oscillations by adrenergic receptor activation in the olfactory bulb. *J Neurophysiol* 99: 2021–2025, 2008.

Gray CM, Freeman WJ, Skinner JE. Chemical dependencies of learning in the rabbit olfactory bulb: acquisition of the transient spatial pattern change depends on norepinephrine. *Behav Neurosci* 100: 585–596, 1986.

Harley C, Darby-King A, McCann J, McLean J. Beta1-adrenoceptor or alpha1-adrenoceptor activation initiates early odor preference learning in rat pups: support for the mitral cell/cAMP model of odor preference learning. *Learn Mem* 13: 8–13, 2006.

Hayar A, Heyward PM, Heinbockel T, Shipley MT, Ennis M. Direct excitation of mitral cells via activation of alpha1-noradrenergic receptors in rat olfactory bulb slices. *J Neurophysiol* 86: 2173–2182, 2001.

Holmberg M, Fagerholm V, Scheinin M. Regional distribution of α_{2C}-adrenoceptor in brain and spinal cord of control mice and transgenic mice overexpressing the α_{2C}-subtype: an autoradiographic study with [3H]RX821002 and [3H]rauwolscine. *Neuroscience* 117: 875–898, 2003.

Jahr CE, Nicoll RA. Noradrenergic modulation of dendrodendritic inhibition in the olfactory bulb. *Nature* 297: 227–229, 1982.

Jiang M, Griff ER, Ennis M, Zimmer LA, Shipley MT. Activation of locus coeruleus enhances the responses of olfactory bulb mitral cells to weak olfactory nerve input. *J Neurosci* 16: 6319–6329, 1996.

Kawaguchi Y, Shindou T. Noradrenergic excitation and inhibition of GABAergic cell types in rat frontal cortex. *J Neurosci* 18: 6963–6976, 1998.

Lewis DA, Campbell MJ, Foote SL, Goldstein M, Morrison JH. The distribution of tyrosine hydroxylase-immunoreactive fibers in primate neocortex is widespread but regionally specific. *J Neurosci* 7: 279–290, 1987.

Linster C, Cleland TA. How spike synchronization among olfactory neurons can contribute to sensory discrimination. *J Comput Neurosci* 10: 187–193, 2001.

Linster C, Gervais R. Investigation of the role of interneurons and their modulation by centrifugal fibers in a neural model of the olfactory bulb. *J Comput Neurosci* 3: 225–246, 1996.

Linster C, Hasselmo M. Modulation of inhibition in a model of olfactory bulb reduces overlap in the neural representation of olfactory stimuli. *Behav Brain Res* 84: 117–127, 1997.

Mandairon N, Peace S, Karnow A, Kim J, Ennis M, Linster C. Noradrenergic modulation in the olfactory bulb influences spontaneous and reward-motivated discrimination, but not the formation of habituation memory. *Eur J Neurosci* 27: 1210–1219, 2008.

McCune SK, Voigt MM, Hill JM. Expression of multiple alpha adrenergic receptor subtype messenger RNAs in the adult rat brain. *Neuroscience* 57: 143–151, 1993.

McLean JH, Shipley MT, Nickell WT, Aston-Jones G, Reyher CKH. Chemoanatomical organization of the noradrenergic input from locus coeruleus to the olfactory bulb of the adult rat. *J Comp Neurol* 285: 339–349, 1989.

Morrison JH, Foote SL, O'Connor D, Bloom FE. Laminar, tangential and regional organization of the noradrenergic innervation of monkey cortex: dopamine-beta-hydroxylase immunohistochemistry. *Brain Res Bull* 9: 309–319, 1982.

Mouly AM, Elaagouby A, Ravel N. A study of the effects of noradrenaline in the rat olfactory bulb using evoked field potential response. *Brain Res* 681: 47–57, 1995.

Nicholas AP, Pieribone VA, Hökfelt T. Cellular localization of messenger RNA for beta-1 and beta-2 adrenergic receptors in rat brain: an in situ hybridization study. *Neuroscience* 56: 1023–1039, 1993.

Okutani F, Kaba H, Takahashi S, Seto K. The biphasic effect of locus coeruleus noradrenergic activation on dendrodendritic inhibition in the rat olfactory bulb. *Brain Res* 783: 272–279, 1998.

Palacios JM, Kuhar MJ. Beta adrenergic receptor localization in rat brain by light microscopic autoradiography. *Neurochem Int* 4: 473–490, 1982.

Pieribone VA, Nicholas AP, Dagerlind A, Hokfelt T. Distribution of α1 adrenoreceptors in rat brain revealed by in situ hybridization experiments utilizing subtype-specific probes. *J Neurosci* 14: 4252–4268, 1994.

Proudfit HK, Clark FM. The projections of locus coeruleus neurons to the spinal cord. *Prog Brain Res* 88: 123–141, 1991.

Ramos BP, Arnsten AF. Adrenergic pharmacology and cognition: focus on the prefrontal cortex. *Pharmacol Ther* 113: 523–536, 2007.

Robbins TW, Everitt BJ. Functional studies of the central catecholamines. *Int Rev Neurobiol* 23: 303–365, 1982.

Sargent-Jones L, Gauger LL, Davis JN. Anatomy of brain alpha1-adrenergic receptors: in vitro autoradiography with [125I]-heat. *J Comp Neurol* 231: 190–208, 1985.

Schuerger RJ, Balaban CD. Organization of the coeruleo-vestibular pathway in rats, rabbits, and monkeys. *Brain Res Brain Res Rev* 30: 189–217, 1999.

Shipley MT, Halloran FJ, de la Torre J. Surprisingly rich projection from locus coeruleus to the olfactory bulb in the rat. *Brain Res* 329: 294–299, 1985.

Sullivan R, Stackenwalt G, Nasr F, Lemon C, Wilson D. Association of an odor with activation of olfactory bulb noradrenergic beta-receptors or locus coeruleus stimulation is sufficient to produce learned approach responses to that odor in neonatal rats. *Behav Neurosci* 114: 957–962, 2000.

Talley EM, Rosin DL, Lee A, Guyenet PG, Lynch KR. Distribution of α2a-adrenergic receptor like immunoreactivity in the rat central nervous system. *J Comp Neurol* 372: 111–134, 1996.

Trombley PQ. Norepinephrine inhibits calcium currents and EPSPs via a G-protein-coupled mechanism in olfactory bulb neurons. *J Neurosci* 12: 3992–3998, 1992.

Trombley PQ. Noradrenergic modulation of synaptic transmission between olfactory bulb neurons in culture: implications to olfactory learning. *Brain Res Bull* 35: 473–484, 1994.

Trombley PQ, Shepherd GM. Noradrenergic inhibition of synaptic transmission between mitral and granule cells in mammalian olfactory bulb cultures. *J Neurosci* 12: 3985–3991, 1992.

Veyrac A, Nguyen V, Marien M, Didier A, Jourdan F. Noradrenergic control of odor recognition in a nonassociative olfactory learning task in the mouse. *Learn Mem* 17: 847–854, 2007.

Wanaka A, Kiyama H, Murakami T, Matsumoto M, Kamada T, Malbon CC, Tohyama M. Immunocytochemical localization of beta-adrenergic receptors in the rat brain. *Brain Res* 485: 125–140, 1989.

Waterhouse BD, Devilbiss D, Fleischer D, Sessler FM, Simpson KL. New perspectives on the functional organization and postsynaptic influences of the locus ceruleus efferent projection system. *Adv Pharmacol* 42: 749–754, 1998.

Wilson DA, Leon M. Noradrenergic modulation of olfactory bulb excitability in the postnatal rat. *Dev Brain Res* 42: 69–75, 1988.

Winzer-Serhan UH, Raymon HK, Broide RS, Chen Y, Leslie FM. Expression of α2 adrenoreceptors during rat brain development-I. α2A messenger RNA expression. *Neuroscience* 76: 241–260, 1997a.

Winzer-Serhan UH, Raymon HK, Broide RS, Chen Y, Leslie FM. Expression of α2 adrenoreceptors during rat brain development-II. α2C messenger RNA expression and [3H]rauwolscine binding. *Neuroscience* 76: 261–272, 1997b.

Woo CC, Leon M. Distribution and development of beta-adrenergic receptors in the rat olfactory bulb. *J Comp Neurol* 352: 1–10, 1995.

Young WS, Kuhar MJ. Noradrenergic a1 and a2 receptors: autoradiographic visualization. *Eur J Pharmacol* 59: 317–319, 1979.

Young WS, Kuhar MJ. Noradrenergic alpha1 and alpha 2 receptors: light microscopic autoradiographic localization. *Proc Natl Acad Sci USA* 77: 1696–1700, 1980.

Yuan Q, Harley CW, Bruce JC, Darby-King A, McLean JH. Isoproterenol increases CREB phosphorylation and olfactory nerve-evoked potentials in normal and 5-HT-depleted olfactory bulbs in rat pups only at doses that produce odor preference learning. *Learn Mem* 7: 413–421, 2000.

Yuan Q, Harley CW, McLean JH. Mitral cell α1 and 5-HT2A receptor colocalization and cAMP coregulation: a new model of norepinephrine-induced learning in the olfactory bulb. *Learn Mem* 10: 5–15, 2003.